Advances in Materials Research, *Vol. 9, No. 1 (2020) 49-62*
DOI: https://doi.org/10.12989/amr.2020.9.1.049

Fracture toughness of amorphus SiC thin films using nanoindentation and simulation

M.A. Mamun [1,2] and A.A. Elmustafa*[1,2]

[1] *Department of Mechanical and Aerospace Engineering, Old Dominion University, 241 Kaufman Hall, Norfolk, VA, USA*
[2] *Applied Research Center-Thomas Jefferson National Accelerator Facility, 12050 Jefferson Ave, Newport News, VA 23606, USA*

(*Received Marcy 25, 2019, Revised February 13, 2020, Accepted March 3, 2020*)

Abstract. Fracture toughness of SiC on Si thin films of thicknesses of 150, 750, and 1500 nm were measured using Agilent XP nanoindenter equipped with a Dynamic Control Module (DCM) in Load Control (LC) and Continuous Stiffness Method (CSM) protocols. The fracture toughness of the Si substrate is also measured. Nanovision images implied that indentations into the films and well deep into the Si caused cracks to initiate at the Si substrate and propagate upward to the films. The composite fracture toughness of the SiC/Si was measured and the fracture toughness of the SiC films was determined based on models that estimate film properties from substrate properties. The composite hardness and modulus of the SiC films were measured as well. For the DCM, the hardness decreases from an average of 35 GPa to an average of 13 GPa as the film thick increases from 150 nm to 1500 nm. The hardness and moduli of the films depict the hardness and modulus of Si at deep indents of 12 and 200 GPa respectively, which correlate well with literature hardness and modulus values of Si. The fracture toughness values of the films were reported as 3.2 $\mathrm{MPa}\sqrt{\mathrm{m}}$.

Keywords: fracture toughness; K_C; nanoindentation; hardness; x-ray diffraction (XRD)

1. Introduction

SiC thin films are sought in high-power and high-temperature applications and in the use of microelectromechanical systems (MEMS) due to their superb mechanical and electrical properties (Mehregany *et al*. 2000, Sarro 2000, Fu *et al*. 2011). SiC exhibits excellent chemical, physical, mechanical and thermal properties with multiple potential applications such as in electronic materials, microwave absorber, furnace heating elements, abrasives, electronic packaging, and heat exchanger (Rafaniello *et al*. 1981). SiC has been recognized as an ideal material for these applications because they possess superior mechanical properties such as hardness, elastic modulus, and fracture toughness (Borrero-Lopez *et al*. 2010, Chen 2012). SiC also possess high resistance to radiation damage due to its small-neutron capture cross section (Snead *et al*. 2007, Swaminathan *et al*. 2010). Another property that makes SiC a high temperature structural material

*Corresponding author, Professor, E-mail: aelmusta@odu.edu
[a] Ph.D., E-mail: mmamu001@odu.edu

http://www.techno-press.org/?journal=amr&subpage=5 ISSN: 2234-0912 (Print), 2234-179X (Online)

is its excellent oxidation, corrosion, and creep properties (Rafaniello *et al*. 1981, Chu *et al*. 2012). It is also noted that for fuel particles in the nuclear industry, SiC coatings are also desirable due to their strong covalent-ionic bonding which produces long term resistance to irradiation and strong mechanical properties (Zhang *et al*. 2012). In order to improve the mechanical properties of SiC such as fracture toughness, hardness, and modulus, it is highly desirable to have some ceramic materials form complete solid solution with SiC. Das *et al*. (2019) produced fine grain Sic-AlN interfacial solid solution layer which helped in crack deflection and improved fracture toughness. Finite element simulations we performed on SiC and low dielectric constant (low K) SiCO based multi-layer films to evaluate the nanoindentation hardness, modulus, and fracture toughness (Deng *et al*. 2019). An interfacial layer is added to the SiCO/SiCN and SiCN/Si to improve the accuracy of the model (Deng *et al*. 2019). The addition of the interfacial layer produced results that correlate well with the experimental data and the mechanical behavior relating to interfacial delamination was successfully captured (Deng *et al*. 2019).

Although SiC films provide a wide range of applications in industries, there are still uncertainties surrounding their resulting mechanical and structural properties specifically hardness, modulus, and fracture toughness measurements. The resulting mechanical properties suffer from proper measurements and accurate determination due to the substrate effect. Therefore, there exists a critical need for examining the hardness, modulus, and fracture toughness of SiC films using nanoindentation technique and simulations to account for the substrate effect. In this research, we examine the hardness, modulus, and fracture toughness of SiC films of thicknesses of 150, 750, and 1500 nm on Si substrate. We use analytical simulations with experimental measurements to properly address the substrate effect especially for the 150 nm film.

We tested three samples of 150, 750, 1500 nm film thickness in addition to a pure silicon sample for the mechanical, structural properties, and fracture toughness. These properties were investigated using nanoindentation. The composite hardness and modulus of the SiC films of thicknesses of 150, 750 and 1500 nm are measured using Agilent XP and DCM II nanoindenter in Continuous Stiffness Method (CSM) and Load Control (LC) protocols respectively. In addition, X-ray diffraction (XRD), and scanning electron microscopy (SEM) were used to investigate the structure and morphology of the films.

Traditional models estimate composite fracture toughness of a film/substrate system and commonly do not provide information about the fracture toughness of the film alone from measurements. In this work, we developed a generalized fracture toughness model to determine fracture toughness of a film independent of the substrate effect. A particular model for SiC thin film is proposed based on the generalized model and we demonstrated the effectiveness by determining the SiC thin film's fracture toughness value independent of the substrate effect. This model covers a wide range of film thicknesses and it is tested for a hard film on a soft substrate such as SiC/Si.

2. Experimental details

Three SiC films were deposited onto prime silicon substrates using an industrial PVD system equipped with a planar magnetron sputter source and 99.99% pure silicon carbide target. The samples were provided by Nanomechanics Inc. of Knoxville, TN. No more details were provided on the preparation of the samples.

To investigate the Hardness and modulus of different SiC films on Si samples, XP CSM DCM

II Basic load control (LC) tests were performed. The CSM test provides the load, hardness, modulus properties as a continuous function of depth of penetration. Each of the XP and DCM II modules uses a separate three-sided diamond Berkovich indenter tip. The XP Standard Hardness, Modulus, and Tip Calibration (SHMTC) in continuous stiffness methods (CSM) method was employed for testing. The SHMTC CSM method generates hardness and modulus results as continuous functions of the penetration depth into the test specimen. This method is used when examining hard materials such as fused silica, glass, ceramic, metals and SiC, which is the subject material of this study. The G-Series DCM II Basic Hardness, Modulus, Tip Cal, Load Control method with 5steps of loading and unloading was employed with maximum load used as 0.5 mN, 5 mN and 10 mN for the SiC samples of 150, 750 and 1500 nm film thickness respectively.

In order to study the fracture toughness, a systematic test approach was followed to measure the crack lengths generated due to indentation made at different maximum loads. A three-sided diamond Cube Corner tip was used for this purpose. A series of displacement-controlled indents using G-Series XP CSM Nanovision Indent and Scan method in NanoSuite was employed to

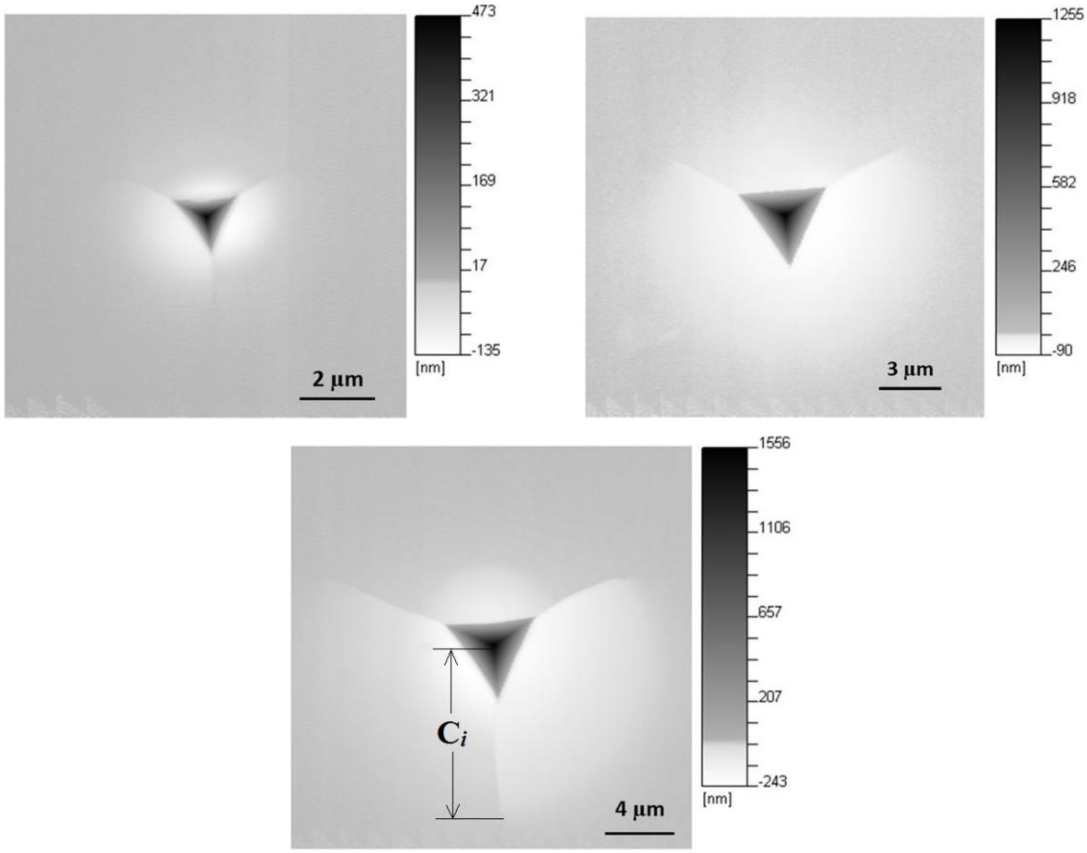

Fig. 1 Residual impression of a cube corner nanoindents using a G-Series XP CSM nanovision Indent and Scan method o5n SiC films on Si substrate: (a) a 750 nm indent on a 150 nm thick film resulting in an average crack length of 2.20 µm, (b) a 1750 nm indent on a 750 nm thick film resulting in an average crack length of 5.96 µm, and (c) a 2300 nm indent on a 1500 nm thick film resulting in an average crack length is 9.71 µm

perform the indents and image the crack length. Nanovision investigation for various depths of indentation suggests that cracks initiate at the film/substrate interface and propagate radially to the surface of the three samples tested. Figs. 1(a)-1(c) depict indents of 750, 1750, and 2300 nm on the 150, 750, and 1500 nm thick films respectively. The crack length, C_i is measured from the center of the indent to the tip of the radial crack as shown in Fig. 1(c). To take into account the substrate effect, modeling and simulations were performed to isolate the films properties from the substrate. The measured crack lengths and the corresponding maximum load were subsequently used for calculating the fracture toughness at different depth (or load).

3. Results and discussion

3.1 XRD results

Fig. 2 shows the X-ray 2Θ diffraction patterns of the cubic three SiC thin films grown onto prime silicon substrates using an industrial PVD system equipped with a planar magnetron sputter source and 99.99% pure silicon carbide target. From Fig. 2, we can see that the 150, 750, and 1500 nm SiC thin films have an amorphous structure.

3.2 Nanoindentation results

Prior to the measurements, the tip was calibrated using a standard fused silica sample. The hardness as a function of depth of indentation normalized to the film thickness is shown in Fig. 3.

The Meyer hardness is defined as the maximum load (from the load-depth curve) over the projected area. The hardness is given by

$$H = \frac{L}{A} \tag{1}$$

where L is the indentation load, and A is the projected contact area. Since the unloading portion

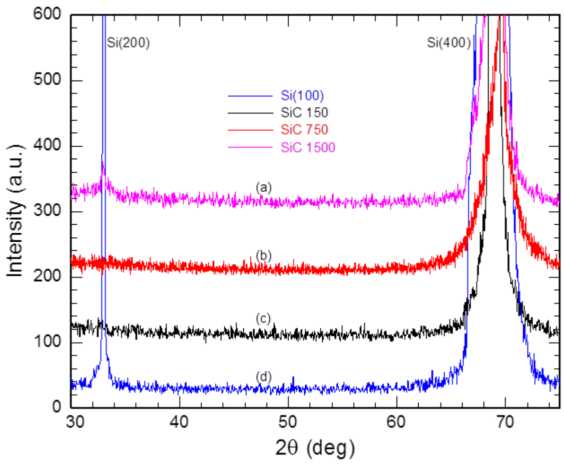

Fig. 2 X-Ray diffraction patterns of 150, 750, and 1500 nm SiC thin films grown on Si(100) substrates

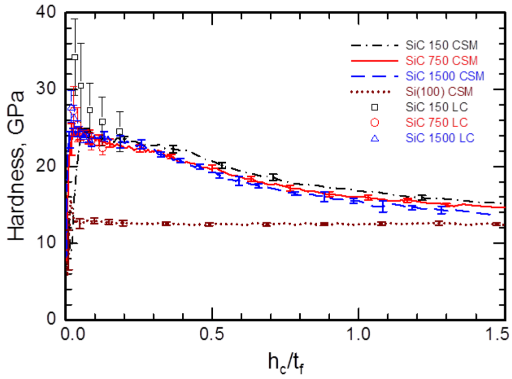

Fig. 3 Hardness versus depth of indentation normalized to the film thickness

of the load-displacement curve is characterized by elastic displacement, it is always possible to determine the elastic modulus of the material being tested from the slope of the unloading curve.

For a uniform specimen, the reciprocal of the slope (the unloading compliance, C) is related to the elastic properties. Therefore, the unloading compliance can be written as (Oliver and Pharr 2004)

$$C = \frac{\sqrt{\pi}}{2 \rightleftarrows \beta \rightleftarrows E_r\sqrt{A}} \tag{2}$$

where β is a constant. β = 1.0 (Oliver and Pharr 2004).

E_r is the reduced modulus defined as

$$\frac{1}{E_r} = \frac{1-\nu_s^2}{E_s} + \frac{1-\nu_d^2}{E_d} \tag{3}$$

E_s and E_d are Young's moduli and ν_s and ν_d are Poisson's ratios of the specimen and the indenter, respectively. The diamond tip Poisson's ratio and modulus are $\nu_d = 0.07$ and $E_d = 1137$ GPa respectively.

From Fig. 3, the measured hardness increases monotonically from an average of 12 GPa for deep indents measured using XP CSM to an average of 25 GPa measured using the DCM II head in LC modules. The average hardness of the Si substrate is 12 GPa which agrees well with reported hardness values of Si from the literature (Mishra *et al*. 2008).

The modulus versus depth of indentation normalized to the film thickness is shown in Fig. 4. There are insignificant variations between the measurement results using the DCM II and the XP head for the 750 and 1500 nm thick films at shallow depth of indentation whereas in the case of the 150 nm thin film, the modulus varies for the CSM and LC due to the high noise level in the CSM at shallow depth of indentation. The average modulus of the film is 420±60 GPa whereas for the substrate the average modulus is 180 GPa, which is considered higher than the average modulus for cubic Si reported in the literature due to pile-up (Mishra *et al*. 2008).

3.3 Fracture toughness from crack length measurements

The fracture toughness, K_C can be determined from the radial crack length measurement using

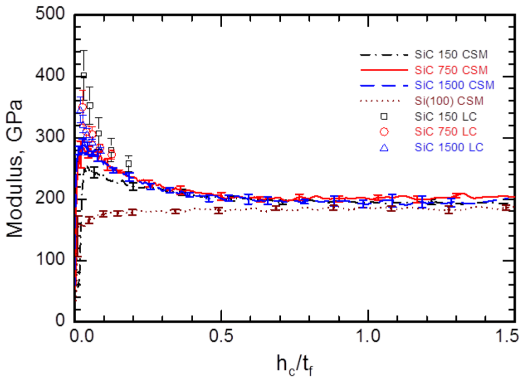

Fig. 4 Modulus versus depth of indentation normalized to the film thickness

the following equation (Lawn *et al*. 1980)

$$K_C = \alpha\sqrt{\frac{E}{H}}\left(\frac{P}{C^{3/2}}\right), \tag{4}$$

where P is the maximum indentation load, E and H are the modulus and hardness of the material, respectively, and α is an empirical constant which depends on the geometry of the indenter (α = 0.04 for a cube-corner tip) (Pharr 1998). We plot the crack length, $C^{3/2}$ versus the maximum load, P in Fig. 5. The lengths increase with increasing the maximum indentation loading for each of the four samples. The SiC 150 nm samples depict early crack emergence for shallow indentation loads whereas the SiC 750 nm and SiC 1500 nm samples experienced crack emergence with indentation loads higher than 100 and 200 mN respectively. This is obvious because cracks initiate at the Si substrate and propagate upward to the films. The average crack lengths were measured by imaging the indentations using Nanovision scanning. In Fig. 6, we plot the fracture toughness versus maximum load divided by the crack length to the 3/2 power from Eq. (2). The data from the four samples collapsed to form a linear relationship. From this plot, the average fracture toughness

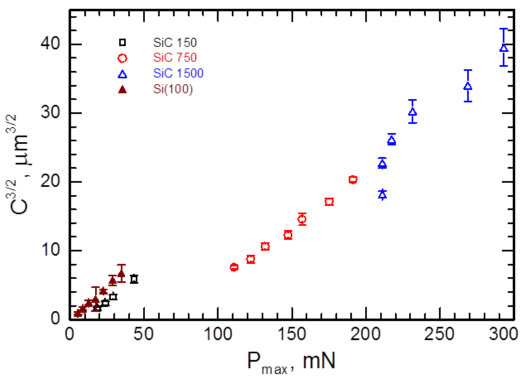

Fig. 5 Crack length to the power 3/2 versus maximum load

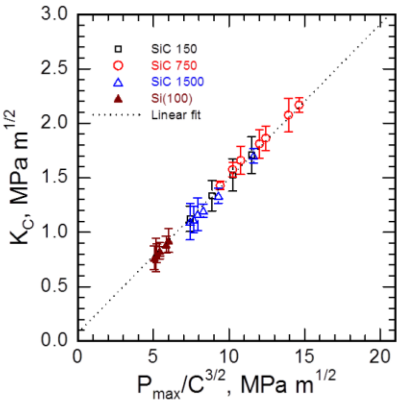

Fig. 6 Fracture toughness versus maximum load divided by the crack length to the power 3/2

of the Si(100) substrate is 0.84 ± 0.08 $\mathrm{MPa}\sqrt{\mathrm{m}}$, which agrees well with literature published values (Pharr 1998). For the SiC 150, 750, and 1500 nm we noticed that the fracture toughness values vary with the maximum applied load due to the Si substrate interaction. This necessitates developing a model to address the fracture toughness of the films independent of the substrate influence.

3.4 Simulation results

To appropriately address the influence of the substrate especially for the 150 nm thin films, we complement the measurements with analytical simulations. It is observed that the radial crack initiates at different depths of indentation which exceeds the film thickness for samples with varying film thickness. Subsequent to penetration into the film and deep into the substrate, cracks emerge on the film's surface suggesting that the substrate influences the measured fracture toughness. The measured fracture strength decreases with the increase of indentation depth and saturates at the substrate demonstrating that the substrate constantly influenced the measured fracture strength as a function of displacement into surface. It is also noted that measured fracture toughness $\mathrm{K_C}$ sharply rise prior to the emergence of the radial cracks suggesting that the cutoff regions of $\mathrm{K_C}$ calculation is based on the occurrence of the radial cracks. For shallower depths of indentation (within 10% of the film thickness) no cracks have been detected. Therefore, it is conceivably that the calculated $\mathrm{K_C}$ might not represent the true fracture toughness of the film. The emergence of the cracks on the surface of the film is dictated by a combination of elastic/plastic deformation of the film and substrate. To accurately estimate the fracture toughness of the film, $\mathrm{K_C^f}$ from the fracture toughness of the composite, $\mathrm{K_C^c}$, and account for the fracture toughness of the substrate, $\mathrm{K_C^s}$, a proper simulation approach must be implemented.

There are several models in the literature that discuss fracture toughness of thin films and coatings. These models can be divided into two groups. In the first group, the fracture toughness is derived from a release energy formulation (Li *et al*. 1997, Xia *et al*. 2004) whereas the second group used the classical fracture toughness method (Zhang *et al*. 2012, Lawn *et al*. 1980, Pharr 1998, Sun and Tong 2007, Anstis *et al*. 1981, Laugier 1985, Mullins *et al*. 2007, Lee *et al*. 2012) . An example of the first group is Li *et al*. (1997) model. Li *et al*. (1997) proposed a fracture toughness model for thin films and coatings based on the release energy rate and approximated the fracture toughness to be dominated by Mode I cracks due to crack opening. The release energy was calculated based on pop-in (step) events during the loading cycle of the load-depth curves in indentation. Zhang and Zhang (2012) concluded that extraction of the release energy from the step is controversial. In our nanoindentation experiments of the SiC films, we have not experienced the pop-in events within the applied maximum loading and therefore based on this we cannot use their energy release model. In second group, several models proposed a fracture toughness model that takes into account the residual stresses and the plastic zone size for thin films (Pharr 1998, Xia *et al*. 2004, Lee *et al*. 2012, Jungk *et al*. 2006, Ponton and Rawlings 1989, Chicot *et al*. 2009). However, to the best of our knowledge no model has been reported so far that calculates the fracture toughness of thin films based on hardness measurements taking into account substrate effects. Therefore, in this work we propose a model to evaluate thin films' fracture toughness from the measured composite fracture toughness.

The literature is rich in models that describe empirical and analytical expressions to isolate thin films' hardness and elastic modulus from the composite hardness and modulus as a function of indentation depth (Maitre *et al*. 2005, Lemoine *et al*. 2007, Pulecio *et al*. 2010, Bhattacharya and Nix 1988, Doerner and Nix 1986, King 1987, Burnett and Rickerby 1987a, b, Jonsson and Hogmark 1984, Gao *et al*. 1992, Stone 1990, Yu *et al*. 1990). The earliest model of the composite film/substrate hardness was proposed by Buckle (1973). Some of the previously cited authors used Buckle's hardness model to expand it to define a model that describes the modulus of elasticity. Buckle's model divides the hardness into two portions based on the boundary conditions. One due to the substrate effect and another one based on the film substrate interaction. The two hardness portions add linearly according to the following relation

$$H_c = H_s + \alpha\left(H_f - H_s\right). \tag{5}$$

The boundary conditions are $\mathrm{H_c = H_s}$ when $\alpha = 0$ at $\mathrm{d_c/t_f} \gg 1$, and $\mathrm{H_c = H_s}$ when $\alpha = 1$ at $\mathrm{d_c/t_f} = 0$; where $\mathrm{H_c}$, $\mathrm{H_f}$, and $\mathrm{H_s}$ represent hardness for the composite, film and substrate respectively. The weight parameter, α is a function of the film thickness ($\mathrm{t_f}$) and the contact depth ($\mathrm{d_c}$) or the displacement into the surface, (h).

Based on Buckle's model, we developed a fracture toughness model that call for the fracture toughness of a film/substrate system and a film/substrate interaction to add linearly. The general form of the model is given below

$$K_C^c = K_C^f + \xi\left\{K_C^s\left(\frac{\nu_f}{\nu_s}\right) - K_C^f\right\}, \tag{6}$$

The boundary conditions are $\mathrm{K_C^c = K_C^f}$, when $\xi = 1$, and ν_f (film's poisson's ratio) $=$ ν_s (substrate Poisson'sration) at $\mathrm{h/t_f} \gg 1$, and $\mathrm{K_C^c = K_C^f}$ when $\xi = 0$ at $\mathrm{h/t_f} = 0$, where $\mathrm{K_C^c = K_C^f}$, and $\mathrm{K_C^s}$ represent fracture toughness for the composite, film and substrate respectively. The weight parameter, ξ is a function of the film thickness ($\mathrm{t_f}$) and the contact depth ($\mathrm{d_c}$) or the displacement into the surface, (h). The weight parameter, ξ is obtained from the best fit to the experimentally measured fracture toughness data and is expressed by the following relation

$$\xi = \frac{\exp^{A\left(\sqrt[n]{x}\right)} - 1}{exp^{A\left(\sqrt[n]{x}\right)} + B}, \tag{7}$$

where $x = h/t_f$ represents the displacement into the surface or the contact depth normalized to the film thickness. The coefficients A and B can be defined in terms of the film and substrate properties as

$$A = \frac{\beta}{n}\left(\frac{H_f}{H_s}\right)^{p_1}\left(\frac{E_s}{E_f}\right)^{q_1}, \tag{8}$$

and

$$B = \frac{1}{n}\left(\frac{H_f}{H_s}\right)^{p_2}\left(\frac{E_s}{E_f}\right)^{q_2}, \tag{9}$$

and therefore ξ can be rewritten as

$$\xi = \frac{\exp^{(Hf/H_s)^2\sqrt{(E_s/E_f)^3}\left(\sqrt[n]{(h/t_f)}/2\pi n\right)} - 1}{exp^{(Hf/H_s)^2\sqrt{(E_s/E_f)^3}\left(\sqrt[n]{(h/t_f)}/2\pi n\right)} + (H\,f/H_s)^2(E_s/E_f)/n} \tag{10}$$

Finally, the fracture strength model for SiC/Si system takes the form

$$K_C^c = K_C^f + \left\{K_C^s\left(\frac{\nu_f}{\nu_s}\right) - K_C^f\right\}\left\{\frac{\exp^{(Hf/H_s)^2\sqrt{(E_s/E_f)^3}\left(\sqrt[n]{(h/t_f)}/2\pi n\right)} - 1}{exp^{(Hf/H_s)^2\sqrt{(E_s/E_f)^3}\left(\sqrt[n]{(h/t_f)}/2\pi n\right)} + (H\,f/H_s)^2(E_s/E_f)/n}\right\} \tag{11}$$

where $\beta, p_1, p_2, q_1,$ and q_2 are fitting parameters whose values are chosen as 1/2π, 2, 2, 3/2, 1 respectively. E_C and E_f are the composite and film elastic moduli. The fitting parameter n is calculated as the ratio of the offset displacement to the film thickness, $n = h_0/t_f$. The offset displacement (h_0) of 116.8, 420, 430 nm used for the 150, 750 and 1500 nm thick SiC films respectively resulted in n values of 0.779, 0.560, 0.287 respectively and resulted in a linear fit for n with film thickness given by Eq. (10) and represented by the plot of Fig. 7

$$n = (-3.6\dot{4} \times 10^{-4})t_f + 0.8\dot{3}. \tag{12}$$

Radial cracks emerged at different penetration depths and propagated from the substrate to the surface for the three SiC films. Fracture occurred when the penetration depth reached 550, 1250, and 1500 nm for the 150, 750, and 1500 nm SiC films respectively. When the crack length is plotted versus the reduced displacement ($x_0 = h - h_0$) the data corresponding to the 150, 750, and 1500 nm films collapsed to a single line represented by a polynomial fit with the Si substrate, Fig. 8. This clearly demonstrates that the cracks initiated at the substrate and propagated upward towards the film.

The fracture toughness weight parameter, ξ quantifies the influence of the substrate on the composite fracture toughness. The parameter, ξ is evaluated using the fitting parameters $\beta, p_1, p_2, q_1,$ and q_2 in addition to the measured hardness and modulus as described by equation 10 and shown in Fig. 9 as a function of displacement into the surface normalized to the film thickness. It is evident that for very thin film such as 150 nm the weight parameter ξ could not

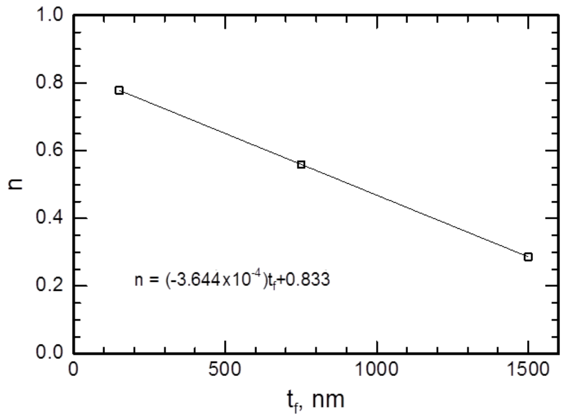

Fig. 7 Offset parameter, n versus film thickness

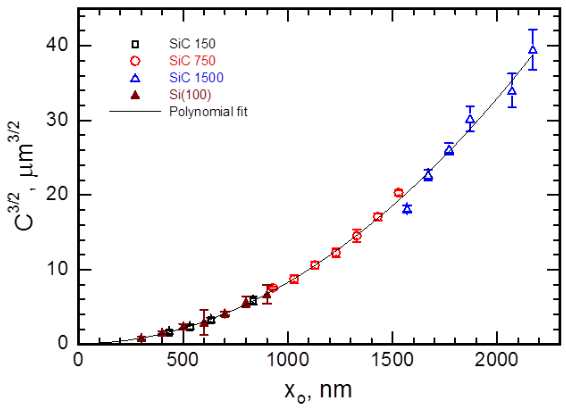

Fig. 8 Crack length to the power 3/2 versus reduced displacement

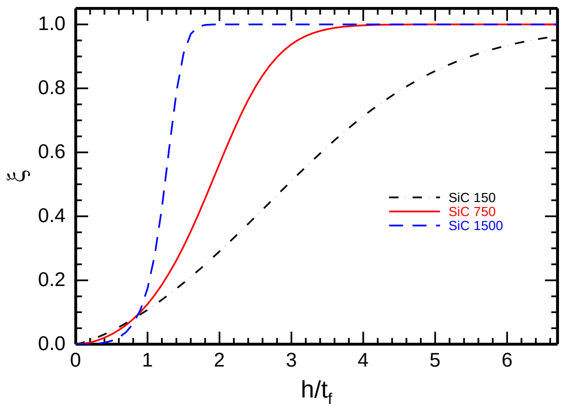

Fig. 9 Fracture toughness weight parameter versus normalized displacement into surface

reach the limiting value of 1 at $h/t_f \gg 1$ because of the severe fracture that affects the actual contact surface area during nanoindentation and ultimately impacted the hardness and elastic modulus.

The fracture toughness of the composite normalized to the fracture toughness of the substrate data are plotted versus the displacement into the surface normalized to the film thickness in Fig. 10. The experimental data are shown in symbols whereas the simulation data are presented in continuous lines. The experimental data were produced using Eq. (4) and the simulation data were generated using Eq. (11). Since the experimentally measured fracture toughness values were calculated based on the composite behavior, therefore the measured hardness and modulus of the composite were used to calculate the fracture toughness as given by Eq. (4). The influence of the substrate on the measured fracture toughness of the composite film/substrate system depends on the film thickness. The proposed fracture toughness model (Eq. (11)) that estimates the fracture toughness from a film/substrate system with known hardness, elastic modulus, and Poisson's' ratio of the film and the substrate demonstrates a capability to capture the trend in the experimental data for a wide range of indentation depth. This model is thus capable of predicting the appropriate fracture toughness values of a film taking into account the influence of the substrate. In other words, one can estimate the fracture toughness for any film thickness on a substrate by fitting the experimentally measured composite fracture toughness data to generate the corresponding, K_C^c as K_C^f when $h = 0$. It can also be noted that the fracture toughness for a film/substrate system will only converge to the substrate's fracture toughness values measured from sufficiently deep indents when $\nu_s = \nu_f$. Fundamentally, the fracture toughness property of the film is independent of the film thickness. However, the higher the film thickness necessitates higher stress level to induce cracks on the film/substrate composite material.

Xia *et al*. 2004 energy-balance-based model also estimates the substrate independent fracture toughness of the film (Xia *et al*. 2004). In this this model, we observe heavy dependence on the residual stress and less contribution of the crack length on the estimation of the fracture toughness values. However, we made an effort to use this model and estimate the fracture toughness values based on our measured crack lengths. This seemed to result in different fracture toughness values for films with different film thickness, the higher the film thickness the higher the fracture toughness values of the film. This indicates that Xia *et al*. (2004) model which is based on microindentation tests with a maximum load of 1 kg on a specific film thickness might require

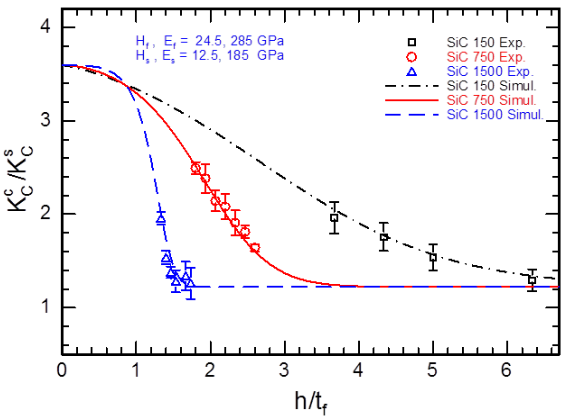

Fig. 10 Normalized fracture toughness versus normalized displacement into surface

more investigation of a film/substrate system with multiple film thickness. Another model that heavily depends on the residual stress to calculate the fracture toughness is Jungk *et al*. (2006) model (Jungk *et al*. 2006). This model also estimates the fracture toughness of a film independent of the substrate effect. We also used this model to predict the fracture toughness values based on our measured crack lengths. Based on this model, the fracture toughness results depict some dependency on the film thickness. Lee *et al*. (2012) demonstrated that the residual stress is already included in Eq. (4) (Lee *et al*. 2012). Therefore, we conclude that the present model is sufficient to accurately predict the fracture toughness of thin films in a film/substrate system with any level of residual stress and a wide range of film thickness using nanoindentation.

4. Conclusions

The influence of the substrate on the measured fracture toughness of the composite film/substrate system depends on the film thickness. However, the fracture toughness property of the film should be independent of the film thickness. We developed a generalized fracture toughness model that integrates experimental and simulation data to predict the fracture toughness of thin films in a film/substrate system. A particular model for SiC thin film is proposed based on the generalized model. This model covers a wide range of film thickness and it is tested for a hard film on a soft substrate such as SiC/Si. The proposed fracture toughness model estimated the fracture toughness values of the SiC films as $3.2 \ \mathrm{MPa}\sqrt{\mathrm{m}}$.

References

Anstis, G.R., Chantikul, P., Lawn, B.R. and Marshall, D.B. (1981), "A critical evaluation of indentation techniques for measuring fracture toughness: I, direct crack measurements", *J. Am. Ceramic Soc.*, **64**, 533-538. https://doi.org/10.1111/j.1151-2916.1981.tb10320.x

Bhattacharya, A.K. and Nix, W.D. (1988), "Analysis of elastic and plastic deformation associated with indentation testing of thin films on substrates", *Int. J. Solids Struct.*, **24**, 1287-1298. https://doi.org/10.1016/0020-7683(88)90091-1

Borrero-López, O., Hoffman, M., Bendavid, A. and Martin, P.J. (2010), "The use of the scratch test to measure the fracture strength of brittle thin films", *Thin Solid Films*, **518**, 4911-4917. https://doi.org/10.1016/j.tsf.2010.04.015

Buckle, H. Ed. (1973), *The Science of Hardness Testing and its Research Applications,* American Society for Materials; Metals Park, OH, USA.

Burnett, P.J. and Rickerby, D.S. (1987a), "The mechanical properties of wear-resistant coatings I: modelling of hardness behavior", *Thin Solid Films*, **148**, 41-50. https://doi.org/10.1016/0040-6090(87)90119-2

Burnett, P.J. and Rickerby, D.S. (1987b), "The mechanical properties of wear-resistant coatings II: experimental studies and interpretation of hardness", *Thin Solid Films*, **148**, 51-65. https://doi.org/10.1016/0040-6090(87)90120-9

Chen, J. (2012), "Indentation-based methods to assess fracture toughness for thin coatings", *J. Phys. D: Appl. Phys.*, **45**, 203001. https://doi.org/10.1088/0022-3727/45/20/203001

Chicot, D., Duarte, G., Tricoteaux, A., Jorgowski, B., Leriche, A. and Lesage, J. (2009), "Vickers Indentation Fracture (VIF) modeling to analyze multi-cracking toughness of titania, alumina and zirconia plasma sprayed coatings", *Mater. Sci. Eng.: A*, **527**, 65-76. https://doi.org/10.1016/j.msea.2009.08.058

Chu, Y., Fu, Q., Li, H., Shi, X., Li, K., Wen, X. and Shang, G. (2012), "Effect of SiC nanowires on the mechanical and oxidation protective ability of SiC coating for C/C composites", *J. Am. Ceramic Soc.*,

95(2), 739-745. https://doi.org/10.1111/j.1551-2916.2011.04979.x

Das, J., Patel, P., Reddy, J.J. and Prasad, V.B. (2019), "Microstructure and mechanical properties of a SiC containing advanced structural ceramics", *Int. J. Refractory Metals Hard Mater.*, **84**, 105030. https://doi.org/10.1016/j.ijrmhm.2019.105030

Deng, J., Liao, N., Zhang, M. and Xue, W. (2019), "Extended finite element analysis of plastic and fracture behaviors of SiC-based multi layer thin film system", *Int. J. Mech. Sci.*, **161-162**, 105017. https://doi.org/10.1016/j.ijmecsci.2019.105017

Doerner, M.F. and Nix, W.D. (1986), "A method for interpreting the data from depth-sensing indentation instruments", *J. Mater. Res.*, **1**, 601-609. https://doi.org/10.1557/JMR.1986.0601

Fu, X.A., Dunning, J.L., Mehregany, M. and Zorman, C.A. (2011), "Low stress polycrystalline SiC thin films suitable for MEMS applications", *J. Electrochem. Soc.*, **158**(6), H675-H680.

Gao, H., Chiu, C.-H. and Lee, J. (1992), "Elastic contact versus indentation modeling of multi-layered materials", *Int. J. Solids Struct.*, **29**, 2471-2492. https://doi.org/10.1016/0020-7683(92)90004-D

Guan, K., Zhang, L., Zhu, F., Li, H., Sheng, H. and Guo, Y. (2020), "Multi-layer SiC-graphene oxide-hydroxyapatite bioactive coating for carbon/carbon composites", *J. Alloys Compounds*, **821**, 153543. https://doi.org/10.1016/j.jallcom.2019.153543

Jönsson, B. and Hogmark, S. (1984), "Hardness measurements of thin films", *Thin Solid Films*, **114**, 257-269. https://doi.org/10.1016/0040-6090(84)90123-8

Jungk, J.M., Boyce, B.L., Buchheit, T.E., Friedmann, T.A., Yang, D. and Gerberich, W.W. (2006), "Indentation fracture toughness and acoustic energy release in tetrahedral amorphous carbon diamond-like thin films", *Acta Materialia*, **54**, 4043-4052. https://doi.org/10.1016/j.actamat.2006.05.003

King, R.B. (1987), "Elastic analysis of some punch problems for a layered medium", *Int. J. Solids Struct.*, **23**, 1657-1664.

Laugier, M.T. (1985), "The elastic/plastic indentation of ceramics", *J. Mater. Sci. Lett.*, **4**, 1539-1541. https://doi.org/10.1007/BF00721390

Lawn, B.R., Evans, A.G. and Marshall, D.B. (1980), "Elastic/plastic indentation damage in ceramics: the median/radial crack system", *J. Am. Ceramic Soc.*, **63**, 574-581. https://doi.org/10.1111/j.1151-2916.1980.tb10768.x

Lee, J.H., Gao, Y.F., Johanns, K.E. and Pharr, G.M. (2012), "Cohesive interface simulations of indentation cracking as a fracture toughness measurement method for brittle materials", *Acta Materialia*, **60**, 5448-5467. https://doi.org/10.1016/j.actamat.2012.07.011

Lemoine, P., Quinn, J.P., Maguire, P.D., Zhao, J.F. and McLaughlin, J.A. (2007), "Intrinsic mechanical properties of ultra-thin amorphous carbon layers", *Appl. Surf. Sci.*, **253**, 6165-6175. https://doi.org/10.1016/j.apsusc.2007.01.028

Li, X., Diao, D. and Bhushan, B. (1997), "Fracture mechanisms of thin film amorphous carbon films in nanoindentation", *Acta Materialia*, **45**, 4453-4461. https://doi.org/10.1016/S1359-6454(97)00143-2

Maitre, N., Camelio, S., Barranco, A., Girardeau, T. and Breelle, E. (2005), "Physical and chemical properties of amorphous hydrogenated carbon films deposited by PECVD in a low self-bias range", *J. Non-Crystal. Solids*, **351**, 877-884. https://doi.org/10.1016/j.jnoncrysol.2005.01.058

Mehregany, M., Zorman, C.A., Roy, S., Fleischman, A.J., Wu C.-H. and Rajan, N. (2000), "Silicon carbide for microelectromechanical systems", *Int. Mater. Rev.*, **45**, 85-108. https://doi.org/10.1179/095066000101528322

Mishra, P., Bhattacharyya, S.R. and Ghose, D. (2008), "Nanoindentation on single-crystal Si modified by 100 keV Cr+ implantation", *Nuclear Instrum. Methods Phys. Res. Section B: Beam Interact. Mater. Atoms*, **266**,1629-1634. https://doi.org/10.1016/j.nimb.2007.12.036

Mullins, L.P., Bruzzi, M.S. and McHugh, P.E. (2007), "Measurement of the microstructural fracture toughness of cortical bone using indentation fracture", *J. Biomech.*, **40**, 3285-3288. https://doi.org/10.1016/j.jbiomech.2007.04.020

Oliver, W.C. and Pharr, G.M. (2004), "Measurement of hardness and elastic modulus by instrumented indentation: Advances in understanding and refinements to methodology", *J. Mater. Res.*, **19**, 3-20. https://doi.org/10.1557/jmr.2004.19.1.3

Pharr, G.M. (1998), “Measurement of mechanical properties by ultra-lowload indentation”, *Mater. Sci. Eng. A*, **253**, 151-159. https://doi.org/10.1016/S0921-5093(98)00724-2

Ponton, C.B. and Rawlings, R.D. (1989), “Vickers indentation fracture toughness test Part 1 Review of literature and formulation of standardised indentation toughness equations”, *Mater. Sci. Technol.*, **5**, 865-872. https://doi.org/10.1179/mst.1989.5.9.865

Pulecio, S.A.R., Farias, M.C.M. and Souza, R.M. (2010), “Finite element and dimensional analysis algorithm for the prediction of mechanical properties of bulk materials and thin films”, *Surf. Coatings Technol.*, **205**, 1386-1392. https://doi.org/10.1016/j.surfcoat.2010.07.039

Sarro, P.M. (2000), “Silicon carbide as a new MEMS technology”, *Sensors Actuat. A: Phys.*, **82**, 210-218. https://doi.org/10.1016/S0924-4247(99)00335-0

Snead, L.L., Nozawa, T., Katoh, Y., Byun, T.S., Kondo, S. and Petti, D.A. (2007), “Handbook of SiC properties for fuel performance modeling”, *J. Nuclear Mater.*, **371**, 329-377. https://doi.org/10.1016/j.jnucmat.2007.05.016

Swaminathan, N., Kamenski, P.J., Morgan, D. and Szlufarska, I. (2010), “Effects of grain size and grain boundaries on defect production in nanocrystalline 3C–SiC”, *Acta Materialia*, **58**, 2843-2853. https://doi.org/10.1016/j.actamat.2010.01.009

Stone, D.S. (1990), “Elastic analysis to aid in extracting thin film elastic moduli from continuous indentation data”, *J. Electronic Packaging*, **112**, 41-46. https://doi.org/10.1115/1.2904339

Sun, J.Y. and Tong, J. (2007), “Fracture toughness properties of three different biomaterials measured by nanoindentation”, *J. Bionic Eng.*, **4**, 11-17. https://doi.org/10.1016/S1672-6529(07)60007-9

Rafaniello, W., Cho, K. and Virkar, A.V. (1981), “Fabrication and characterization of SiC-AlN alloys”, *Journal of Materials Science*, **16**, 3479-3488. https://doi.org/10.1007/BF00586311

Xia, Z., Curtin, W.A. and Sheldon, B.W. (2004), “A new method to evaluate the fracture toughness of thin films”, *Acta Materialia*, **52**, 3507-3517. https://doi.org/10.1016/j.actamat.2004.04.004

Yu, H.Y., Sanday, S.C. and Rath, B.B. (1990), “The effect of substrate on the elastic properties of films determined by the indentation test-axisymmetric Boussinesq problem”, *J. Mech. Phys. Solids*, **38**, 745-764. https://doi.org/10.1016/0022-5096(90)90038-6

Zhang, S. and Zhang, X. (2012), “Toughness evaluation of hard coatings and thin films”, *Thin Solid Films*, **520**, 2375-2389. https://doi.org/10.1016/j.tsf.2011.09.036

Zhang, H., López-Honorato, E., Javed, A., Zhao, X., Tan, J. and Xiao, P. (2012), “A study of the microstructure and mechanical properties of SiC coatings on spherical particles”, *J. Eur. Ceramic Soc.*, **32**, 1775-1786. https://doi.org/10.1016/j.jeurceramsoc.2011.12.014

CC